Istituto Nazionale di Geofisica e Vulcanologia

SECOND SUMMARY REPORT ON THE M_L 6.0 AMATRICE EARTHQUAKE OF AUGUST 24, 2016 (CENTRAL ITALY)

INGV Working Group on the Amatrice Earthquake

September 19, 2016

Cite as: INGV working group on the Amatrice earthquake (2016). *Second summary report on the M6.0 Amatrice earthquake of August 24, 2016 (Central Italy), doi: 10.5281/zenodo.166241*

INDEX

Introduction

About four weeks have passed since the local magnitude Ml 6.0 (moment magnitude Mw 6.0) earthquake struck the central Apennines area, between the towns of Norcia an Amatrice, on August 24. The amount of data so far collected and the ongoing studies, allow for a more detailed knowledge of the processes behind the earthquake and its seismic sequence.
In the following we will illustrate analyses and results that integrate the ones described in the "First Summary Report on the Amatrice Earthquake".

1 Seismic sequence

1.1 Seismic monitoring networks (SISMIKO and Emersito emergency groups)

The good density and coverage of the National Seismic Network (RSN) in the epicentral area (blue triangles in Figure 1.1-1), allowed for an accurate calculation of the epicentral coordinates and magnitude of the main Ml 6.0 (Mw 6.0) event on August 24 at 03:36 (CEST) and of the aftershocks that followed in the in the first few hours. Naturally, to obtain more accurate hypocentral locations, in particular the depth coordinate, it is necessary to increase the seismic network density. To this end, the coordination group decided to install 17 additional INGV temporary stations (SISMIKO). The first ones deployed started recording on the morning of the August 24, while other stations were installed in the following days (12 of the stations are used for real time monitoring, the other 5 are used in the revision stage for the compilation of the Italian Seismic Bulletin).

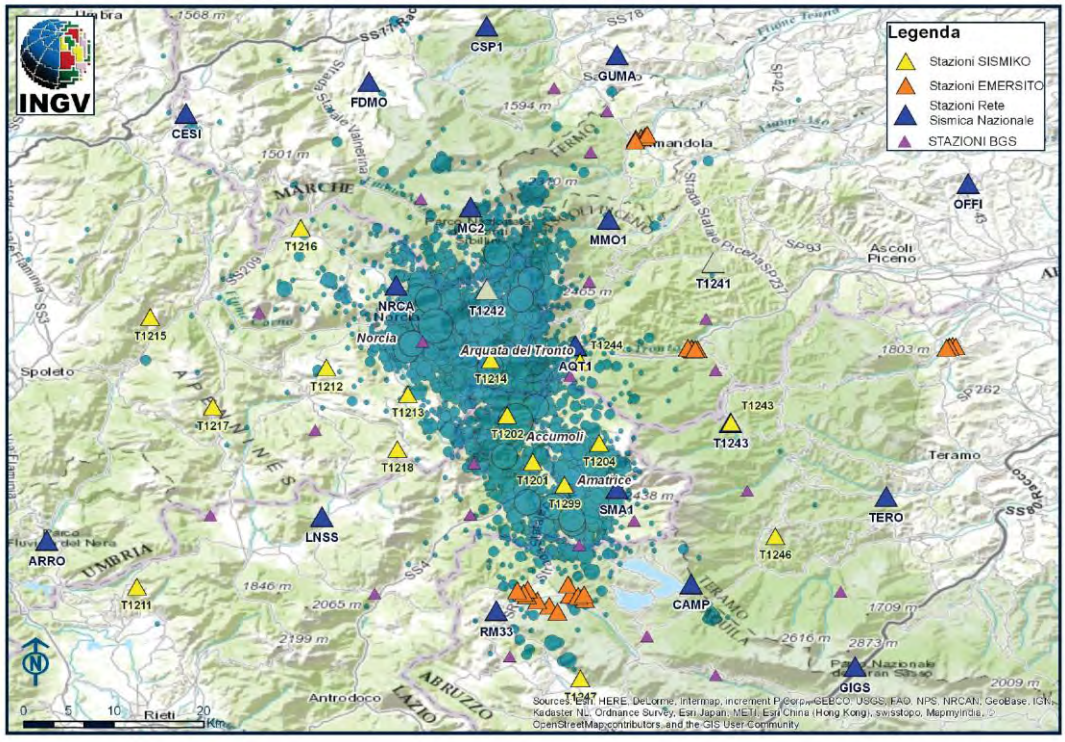

Figure 1.1-1. Map of the INGV seismic network in the epicentral area; the temporary stations (yellow and gray triangles) were installed between the 24th and 28th of August 2016 to integrate the RSN (blue triangles). In addition, the EMERSITO stations were installed (orange triangles). The map also shows

broadband stations that were deployed in collaboration with the British Geological Survey (BGS; small fuchsia triangles).

Data recorded by the temporary stations and by the RSN are available from the EIDA archive (*European Integrated Data Archive*; Figure 1.1-2).

Figure 1.1-2. Data recorded by the temporary stations and by the RSN stations in continuous mode, are available through access to the EIDA site (http://145.23.252.222/eida/webdc3/index.html).

Other stations were added to the ones that were previously installed to improve earthquake locations. The emergency group EMERSITO (a task force that includes personnel from different INGV sections and is dedicated to the study of earthquake site effects) selected, during the first emergency phase (August 24-25), several sites near the epicentral area. The sites were chosen within easily accessible urban areas where there are particular structural and geological conditions (i.e., topography, fault zone, basin) that could cause site effects. Overall, 22 stations were installed (orange triangles in Figure 1.1-1), of which 5 are in real-time acquisition (one of them is used for hypocentral locations by the surveillance system). The stations are divided in 4 seismic networks in the towns of Amandola (FM; Figure 1.1-3), Civitella del Tronto (TE), Montereale (AQ), and Capitignano (AQ).

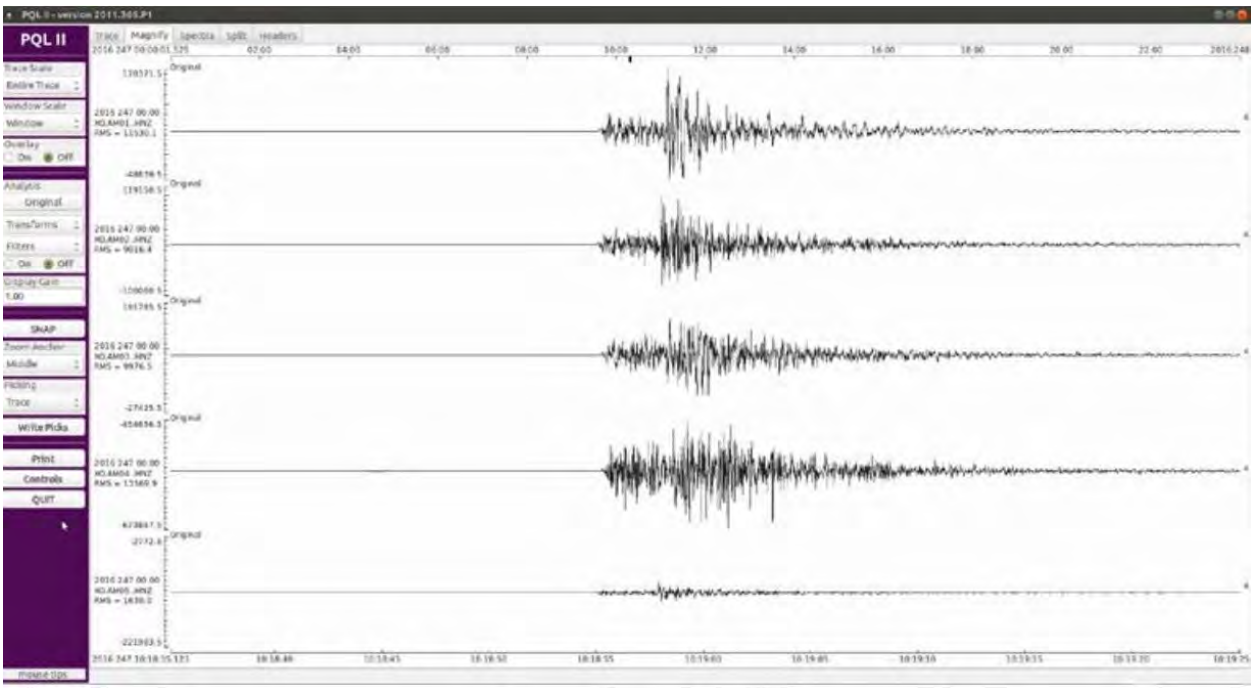

Figure 1.1-3. Traces (vertical component) from an Mw 4.3 recorded at 10:18 UTC on September 3 2016 by the 5 accelerometers installed at Amandola .

The stations were installed in the days of August 26-31 and will be moved to other areas in the second half of September, in agreement with the Seismic Microzonation Center.
In adition to INGV, several other national an international institutions have installed temporary networks. In particular, the Italian Civil Protection Department (DPC) has installed a few accelerometric stations to complement the National Accelerometric Network (RAN), and the *British Geoligical Survey* (BGS) has installed in the past week several broadband (BB) seismic stations.

1.2 Evolution of the seismic sequence

The over 9000 aftershocks that have been located up to September 16, 2016 (ISIDe working group (2016) *version* 1.0, DOI: 10.13127/ISIDe; cnt.rm.ingv.it), are distributed within a crustal volume that occupies a surface that is more extended than the area struck in the first few days, roughly comprised between the townships of Norcia and Amatrice. At the time of writing this second report, the surface area affected by the seismic sequence has an extension of about 50 km in the Apenninic direction (from the town of Ussita in the north, to the lake of Campotosto in the south), and about 15 km in the perpendicular direction (Figure 1.2-1).

In the northern area, near the town of Norcia, the seismic sequence seems to have extended to portions of the fault system that are NE with respect to the part activated at the beginning of the sequence. In the same area the last Ml > 4.0 took place on September 3; three additional events of Magnitude ~ 4.0 occurred on September 15 in the area of Norcia.

The overall distribution the sequence's events shown on map (Figure 1.2-1) suggests an activation of a fault system that is oriented along the Apenninic direction. This fault system shows some complexity, particularly in its northern part where the spatial distribution of the aftershocks implies the role of several fault sections.

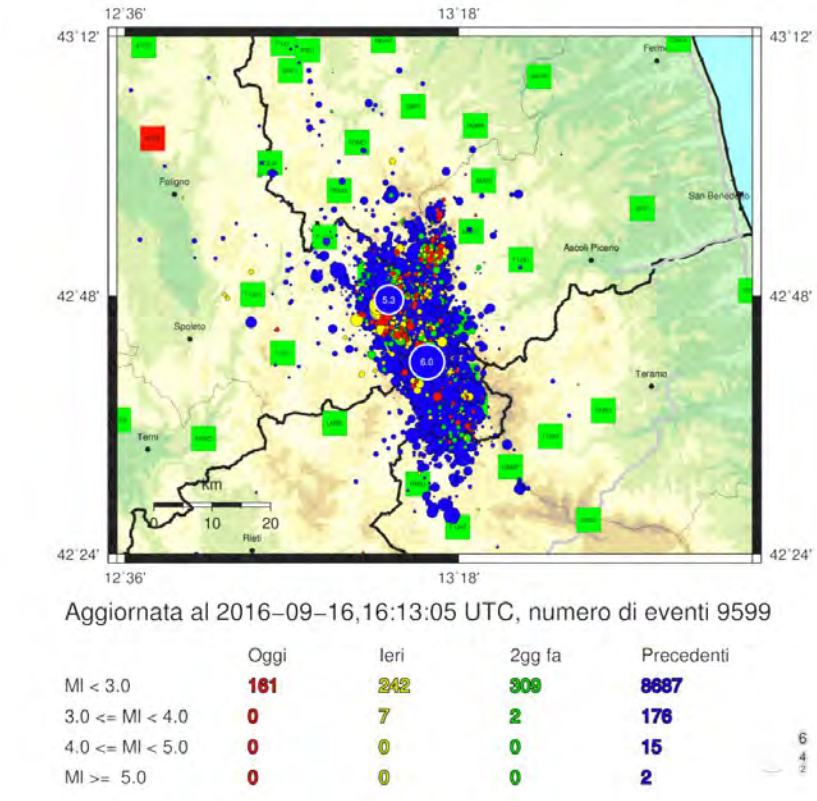

Figure 1.2-1. Epicentral distribution of the sequence (updated to September 16, 2016).

We observe a reduction in time, as the sequence progresses, of the seismicity rate and seismic moment release. The daily number of aftershocks with Ml > 2.0, that was between 200 and 300 in the first days following the mainshock, have gradually decreased down to below 50 in the final days considered in this report (up to September 16), as shown in Figure 1.2-2. On September 15 there was an overall renewal of the activity in the Norcia area that produced several small events, but also 7 earthquakes of magnitude greater than 3.0, an unprecedented occurrence in the previous days. Similarly, the daily seismic moment release, which had gradually decreased up to that moment, increased significantly on the September 15. At the same time it is noteworthy that this increase of the seismic moment release is two orders of magnitude smaller that the one observed right after the mainshock. These simple statistical observations cannot allow us to exclude the future occurrence of earthquakes with relevant magnitude (Ml > 5). In fact, the probability for the occurrence of such events has been estimated to be about 3% by the weekly forecasts that INGV calculates on the basis of the OEF_Italy model [described in W. Marzocchi, A.M. Lombardi, E. Casarotti (2014); The establishment of an operational earthquake forecasting system in Italy. Seismol. Res. Lett., 85(5), 961-969].

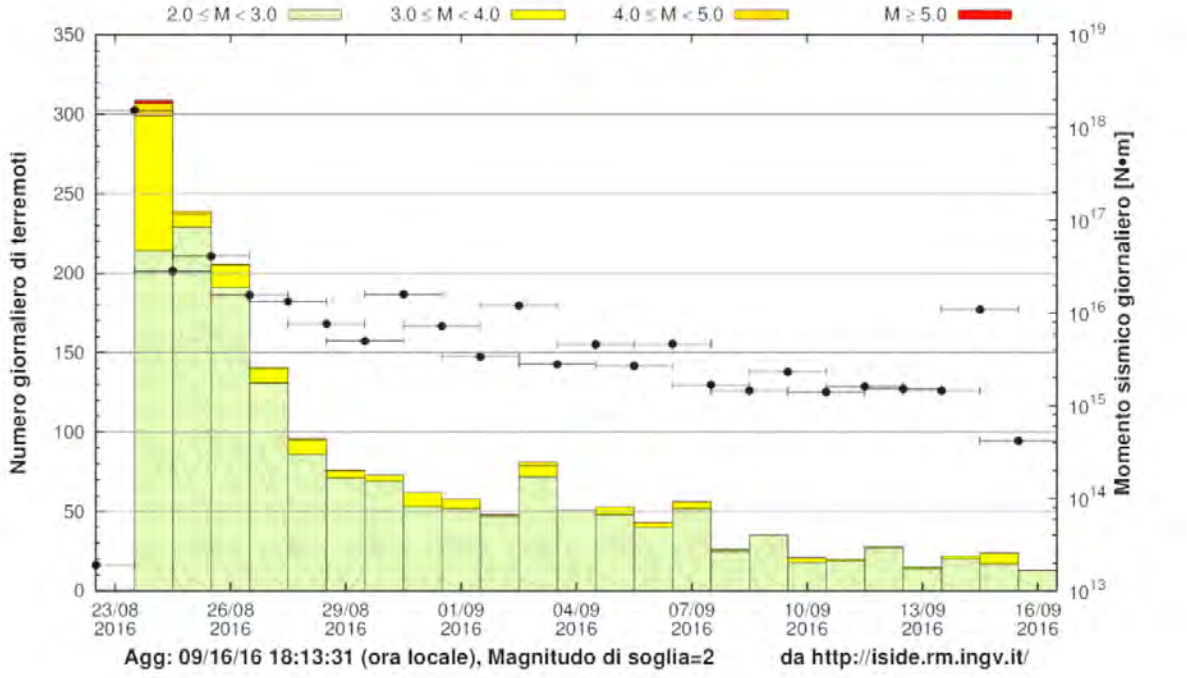

Figure 1.2-2. Histogram of the number of daily events (with M ≥ 2.0) located by INGV. The different colors represent different magnitude classes. The scale to the right refers to the daily seismic moment release.

1.3 Fault geometry derived from hypocenter locations (AMA_LOC Working Group – DOI: 10.5281/zenodo.61404)

Through the analysis of the hypocenter locations we can have a first insight on the geometry of the fault system involved in the seismic sequence. Although this is a preliminary view, as the sequence is still ongoing, it is a useful step to identify more refined studies for the future.

The catalog considered in this analysis is composed of about 3200 earthquakes that occurred between the August 24 and September 3. The events were located with the *NonLinLoc* code (*http://alomax.free.fr/nlloc/*), by inverting the P and S arrival times estimated by the INGV seismic surveillance room personnel and extracted from the INGV database (*http://webservices.rm.ingv.it/fdsnws/event/1/*). The seismic velocity model used for the locations has been published [Carannante et al., 2013]. Locations were selected on the basis of the following criteria:

Rms < 0.5 s; Minimum number of phases = 10; Gap < 180°; Vertical Err < 2 km; Horizontal Err < 1 km

The following figures show several vertical profiles (together with a map showing the location of the profile's trace) across the crustal volume containing the seismic sequence.

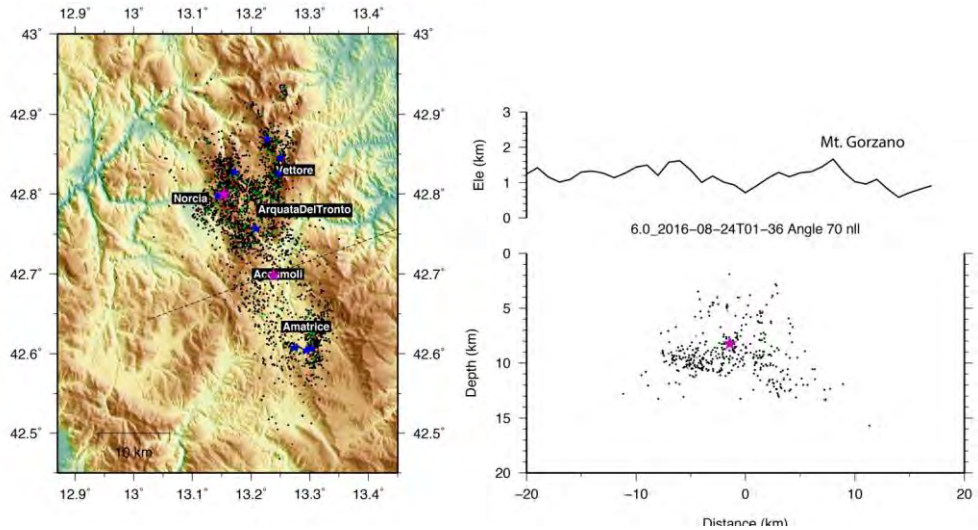

Figure 1.3-1. Map of the relocated epicenters of the seismic sequence and profile along the line shown in the map. The profile includes the M 6.0 mainshock.

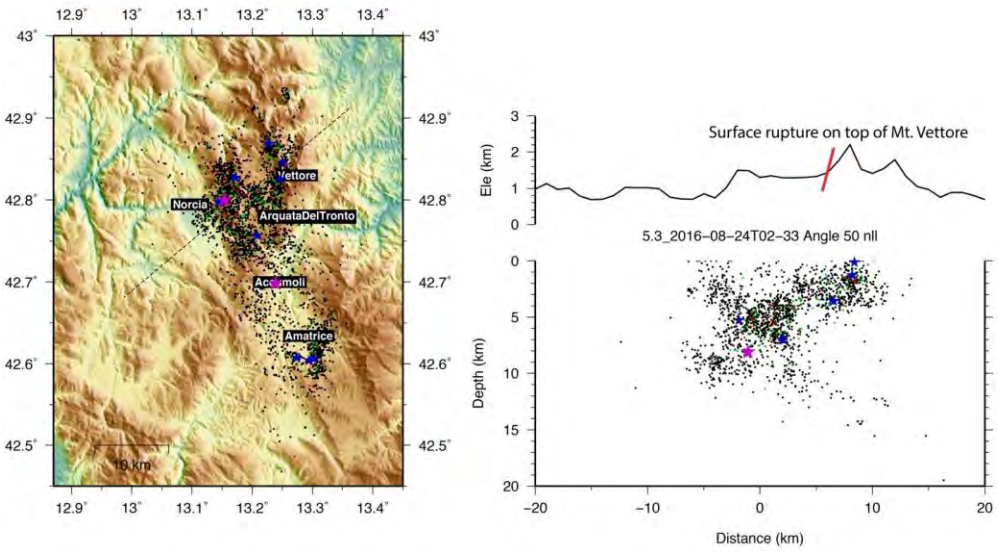

Figure 1.3-2. Map of the relocated epicenters of the seismic sequence and profile along the line shown in the map. The profile crosses the northern part of the crustal volume containing the sequence and includes the largest, Ml 5.3, aftershock.

The profile in Figure 1.3-1 goes through a plane that includes the mainshock (ML 6.0) of August 24 (purple star). This profile is along a direction that is perpendicular to the fault plane strike as derived from the calculated focal mechanism (N156°E, from the INGV-TDMT solution). The spatial distribution of seismicity suggests the possible fault plane were the mainshock originated. This plane, dipping SW, contains at its base, at about 8 km depth, the Ml 6.0

earthquake. The completeness of the catalog so far examined does not allow a more accurate definition of the fault geometry.

The profile in Figure 1.3-2 shows a main plane dipping SW, with an inclination of 40°-45°, and a conjugate system dipping in the opposite way. The more superficial seismic cloud in the eastern sector lies along a N-S direction and includes 3 events with M4+. This seismicity is probably linked with the old thrusting of the Sibillini Mountains outcropping near the easternmost part of the profile. Furthermore, there is deeper seismicity east of the main fault. The trace of the profile is along a plane containing the Ml5.3 event (purple star). This event occurred about one hour after the mainshock at a distance of about 10 km, within the northern part of the crustal volume affected by the seismic sequence. The profile also intersects the area (identified with a red line on the profile) where the EMERGEO group has mapped a series of surface ruptures along the Mt. Vettore fault (Paragraph 2.3.1).
However, the role of the Ml5.3 earthquake in activating the main or conjugate fault planes identified in this profile, is not clear.

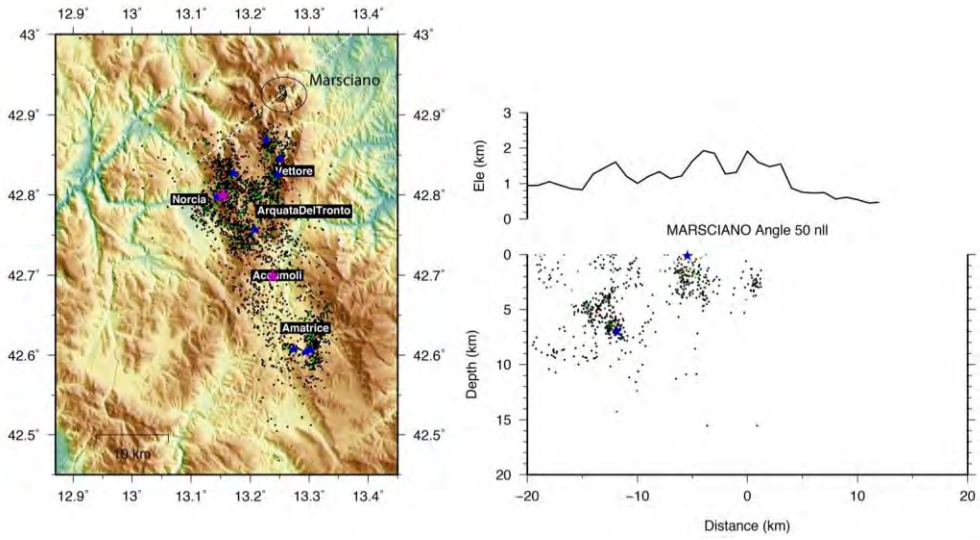

Figure 1.3-3. Map of the relocated epicenters of the seismic sequence and profile along the line shown in the map. The profile crosses the northernmost part of the crustal volume affected by the sequence.

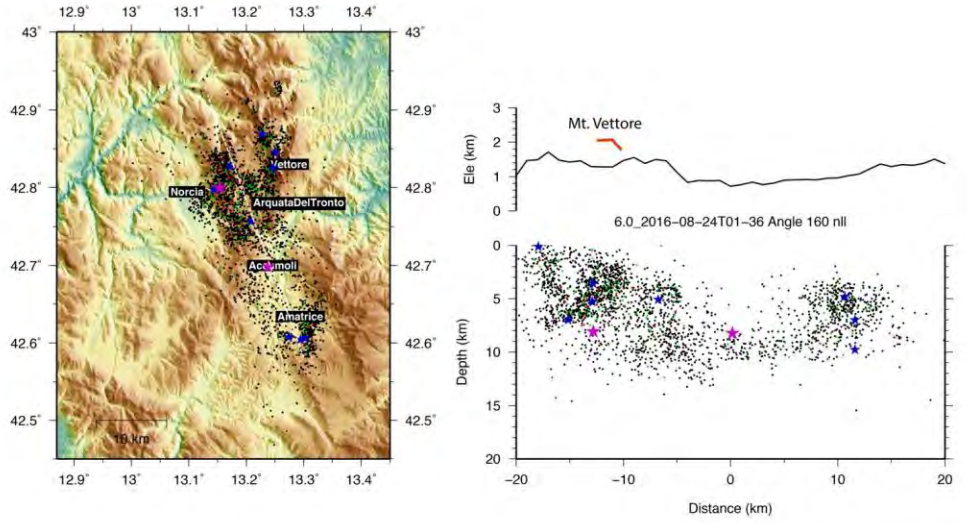

Figure 1.3-4. Map of the relocated epicenters of the seismic sequence and profile along the line shown in the map.

The profile in Figure 1.3-4 was chosen along a direction that is near-parallel to the strike of the mainshock fault plane, to better identify the extension of the crustal volume affected by the seismic sequence. This crustal volume extends about 50 km in the Apenninic direction and goes from the surface down to 10-12 km depth. It is worthy of notice that seismicity is not uniformly distributed along the profile plane, and that scarce seismicity is present is an area between the mainshock hypocenter and the surface. This area corresponds to the part of the fault that underwent the greatest amount of slip during the mainshock, as shown by the static and kinematic inversion results.

1.4 Focal mechanisms (DOI 10.5281/zenodo.61460).

The focal mechanisms calculated for the main aftershocks of the sequence are generally coherent with the tectonic framework of the Apennines and consistent with the fault kinematics that resulted from the main event of August 24 (Ml6.0). Figure 1.4-1 shows the focal mechanisms of the mainshock and of the sequence events with magnitude Ml ≥ 4.0 (focal mechanisms of earthquake with Ml < 4.0 have also been calculated and can be viewed at http://cnt.rm.ingv.it/tdmt). These focal mechanisms are consistent with an extensional kinematics, with minimum stress axis (representing extension) oriented perpendicular to the Apenninic chain axis, *i.e.*, NE-SW. In the eastern part of the crustal volume affected by the seismic sequence we find an Ml 4.3 event with a focal mechanism that points to strike-slip (transcurrent) kinematics. In the same area there is another event (Ml 4.2), which is consistent with extensional kinematics and has focal planes that are along the NNE-SSW direction. These observations, together with the spatial distribution of seismicity, confirm the possible presence of ramifications and greater geometric complexity for the northernmost part of the fault system activated during the sequence (Figure 1.3-3).

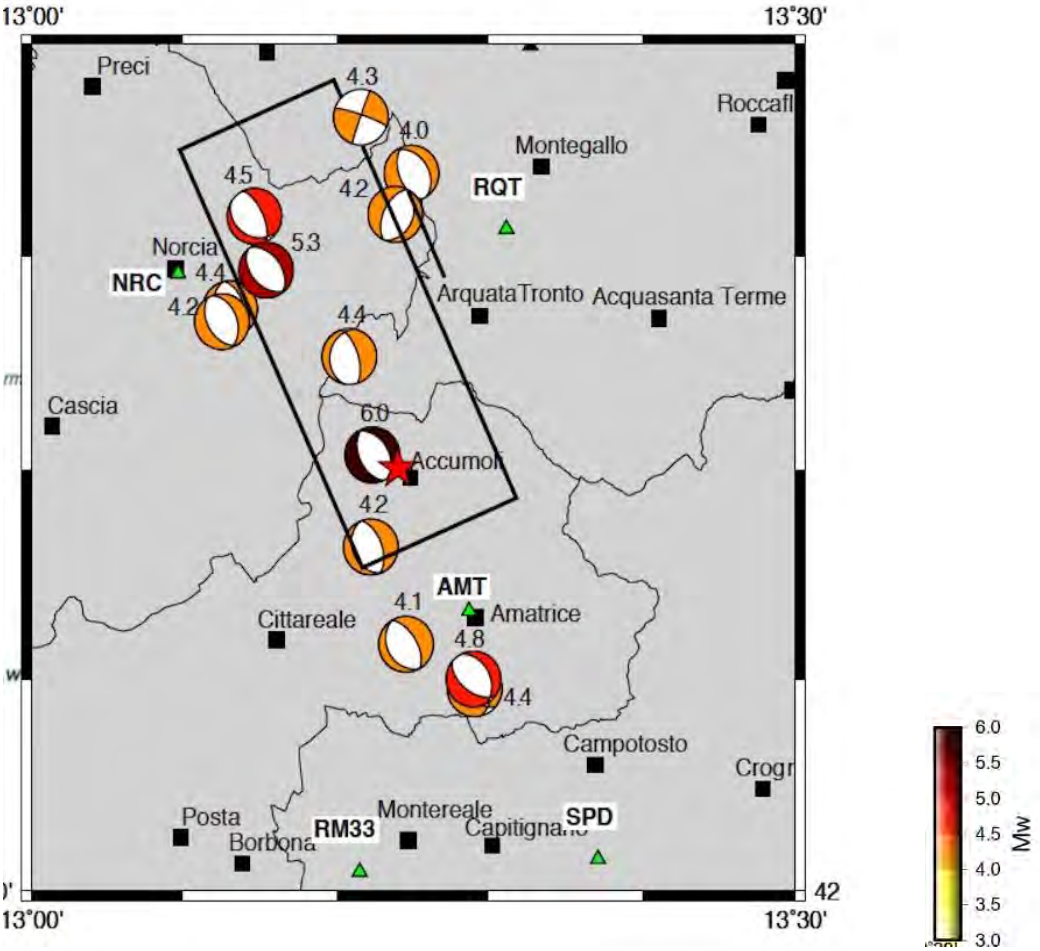

Figure 1.4-1. Focal mechanisms (http://cnt.rm.ingv.it/tdmt) of the main events ($M_L \geq 4.0$) of the sequence (DOI 10.5281/zenodo.61460). On the same web page it is also possible to view solutions for events with smaller magnitudes. Other moment tensor solutions, also alternate solutions for the same events, are available in the Quick Regional CMT Catalogue (http://autorcmt.bo.ingv.it/quicks.html).

2 Main event: available data and analysis

2.1 Strong motion data (INGV: ITACA-ESM Working Group,1 SHAKEMAP working group.2)

About 200 accelerometric waveforms were processed manually, through the procedure of Paolucci et al. [2011], to estimate peaks in acceleration, velocity, and displacement generated by the mainshock, and to measure the duration of the shaking at the different observation sites.

The corrected accelerograms and related information are available in the INGV *Strong-Motion* database (*http://esm.mi.ingv.it*). The original data from the RAN DPC network is available at the web address *http://ran.protezionecivile.it/IT/index.php?evid=340867*, while data from the INGV network is available at EIDA (http://www.orfeus-eu.org/data/eida/). EIDA also distributes data from the University of Genova, the University of Trieste, OGS, AMRA, and from other institutions.

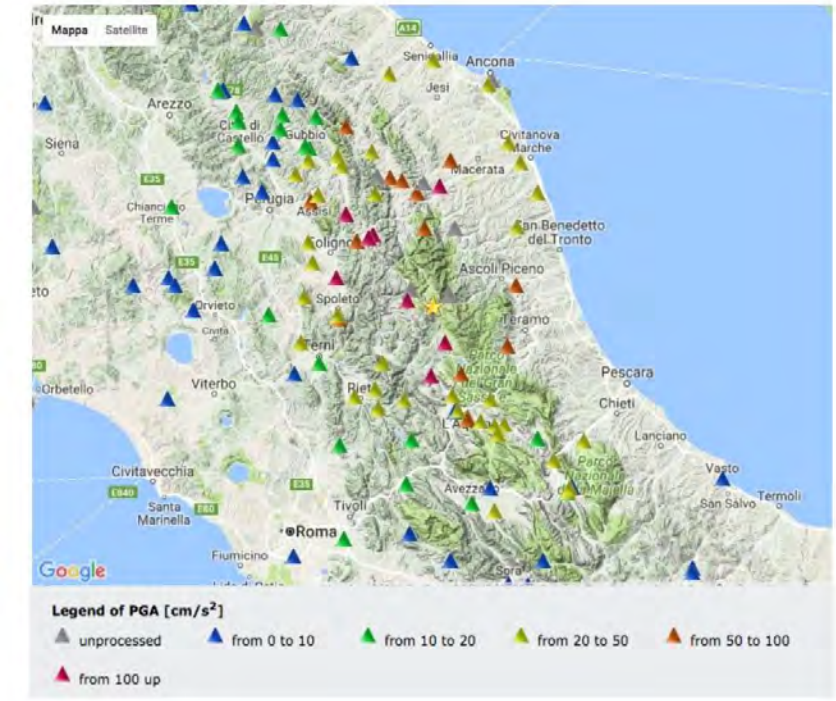

Figure 2.1-1. The map shows the accelerometric stations within a radius of 200 km from the epicenter (yellow star). Triangles represent stations and their color the PGA value (in gal) measured at the site.

Accelerometric data recorded in the first minutes following the mainshock of August 24, were also used to generate *ShakeMaps*. With *ShakeMaps* it is possible to quickly visualize on a map the level of shaking in a region struck by an earthquake. INGV has been calculating *ShakeMaps* for several years, also for earthquakes of moderate magnitude (Ml = 3.0) http://shakemap.rm.ingv.it ; http://cnt.rm.ingv.it/help#impatto). *ShakeMaps* report the peak values recorded by accelerometers (most of them are part of the RAN-DPC and the RSN -INGV networks) located within the region affected by the earthquake. One should keep in mind that *ShakeMaps* are generated starting from point-wise observations at the site where the accelerogram is recorded. The point-wise observations are then interpolated on the basis of a code that takes into account region-specific laws that define how shaking attenuates with distance. Thanks to this procedure it is possible to obtain a continuous representation of the value of shaking in an extended region of interest (Figure 2.1-2).

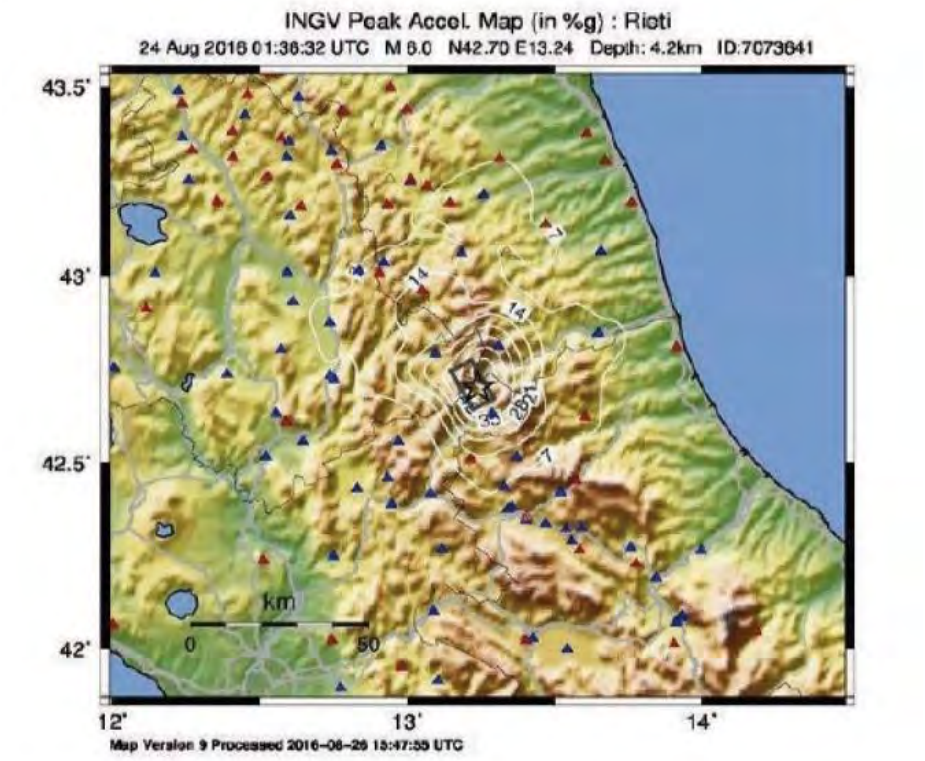

Figure 2.1-2. ShakeMap for the peak horizontal acceleration of the main event (http://shakemap.rm.ingv.it/shake/7073641/intensity.html). Peak values of shaking were observed at the Arquata del Tronto, Norcia and Amatrice stations; this pattern suggests a bi-lateral rupture of the fault (from NW towards SE).

2.1.1 Inversion of Strong Motion data (DOI 10.5281/zenodo.61460)

Detailed information on the source kinematics of the August 24 earthquake (M_L 6.0) was obtained by inverting the accelerometric data from 24 stations located within 42 km from the epicenter (green triangles in Figure 2.1-1). The inversion was performed with the "*non-negative least-squares inversion"* method [Dreger and Kaverina, 2000]. In this method accelerograms are integrated in the time domain and bandpass filtered between 0.02 and 0.5 Hz. The Green's functions are calculated using the CIA velocity model [Hermann et al., 2011]. The fit between the observed and the synthetic accelerograms is shown in Figure 2.1-1.

The inversion procedure provides information on the rupture process: there are two main rupture areas (yellow-red areas in the lower panel of Figure 2.1-1), the first one above (along the fault inclination) and the second NW of the nucleation point; the rise time varies between 0.6 and 2 s; the rupture speed is comprised between 2.0 and 3.5 km/s; the rake (direction of the movement on the fault plane) is heterogeneous in different parts of the fault and it varies between -65° and -105° (blue arrows in the lower panel of Figure 2.1-1); the duration of the rupture was about 8 s.

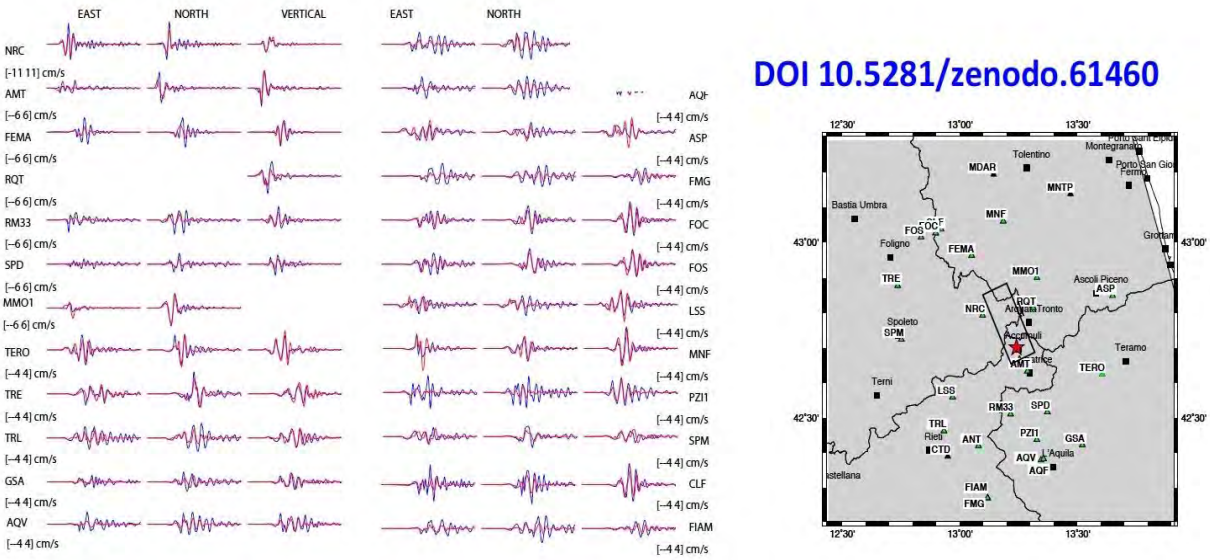

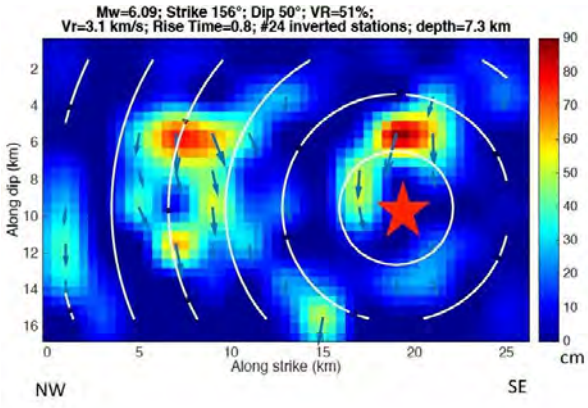

Figure 2.1.-1. Upper-left panel: accelerometric recordings after integration and filtering (in blue), and synthetic traces derived from modeling (in red). Upper-right panel: map with stations; the green triangles represent stations used for the inversion. Lower-left panel: the model shows two main rupture areas on the fault plane, one above and the other NE of the hypocenter.

2.2 Geodesy

2.2.1 GPS data (INGV Working group "GPS Geodesy (GPS data and data analysis center)" DOI 10.5281/zenodo.61355)

The permanent deformation of the Earth's crust caused by the August 24 earthquake was measured by GPS stations located in central Italy. These stations are part of INGV's Rete Integrata Nazionale GPS (RING), and of networks belonging to ISPRA, and DPC (Figure 2.2-1). There are also temporary GPS benchmarks, such as INGV's CA-GeoNetand and IGM95 (Figure 2.2-1). Other GPS data were available from the GNSS networks of Regione Abruzzo, Regione Lazio, ItalPos, NetGeo, Regione Umbria, ASI ed Euref.

The ground displacements recorded by the stations were analized at INGV through processing with the *Bernese*, *Gamit* and *Gipsy* software. Outputs from the different codes were subsequently combined to obtain a single final result. Displacements are calculated by comparing the (daily) positions of the stations in the days preceding the earthquake with the (daily) positions in the days following the earthquake. With this procedure it was possible to calculate the maximum displacement at each station, including the one at Amatrice, the closest to the epicenter of the August 24 shock, with a maximum error of a few millimeters. The largest displacement, 2.5 cm in the NW direction and 1.5 cm of land surface lowering, was in fact measured at Amatrice (station AMAT). The stations at Norcia (NRCI) and Leonessa (LNSS) recorded, respectively, a displacement of 2.4 cm and 2.3 cm towards SW, while Ascoli (ASCC) recorded 1.4 cm towards NE.

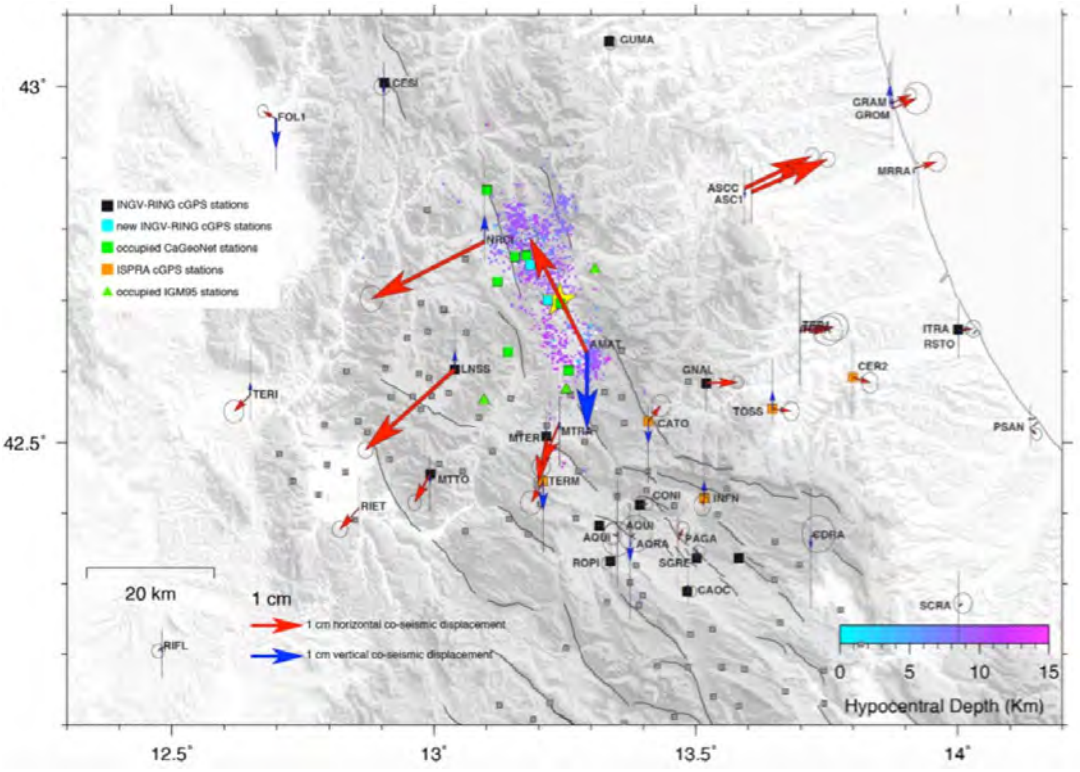

Figure 2.2-1. Coseismic horizontal (red arrows) and vertical (blue arrows) displacements measured by the permanent and temporary GPS stations. Permanent stations: RING-INGV (black and light blue squares); ISPRA and Dipartimento di Protezione Civile (DPC) (orange squares). Temporary stations: CA-GeoNet benchmarks being determined (green squares); IGM95 benchmarks (green triangles). Other GPS data were provided by the following networks: Regione Abruzzo, Regione Lazio, ItalPos, NetGeo, Regione Umbria, ASI ed Euref. The yellow star represents the epicenter of the M6.0 03:36 (CEST), August 24, 2016 earthquake.

2.2.2 Inversion of GPS data (GPS working group doi:10.5281/zenodo.61690)

A preliminary analysis, based on the GPS stations operating during the mainshock, shows that the earthquake was generated by an 18 km long fault running along a NNW-SSE direction and dipping about 50 degrees in the West direction below the Apennines (Figure 2.2-2). The greatest amount of slip (70 cm) is found on the fault section located North of the hypocenter (Figure 2.2-2). The movement of this fault has caused about 3-4 cm extension of the Apenninic chain, between the Tyrrhenian and the Adriatic.

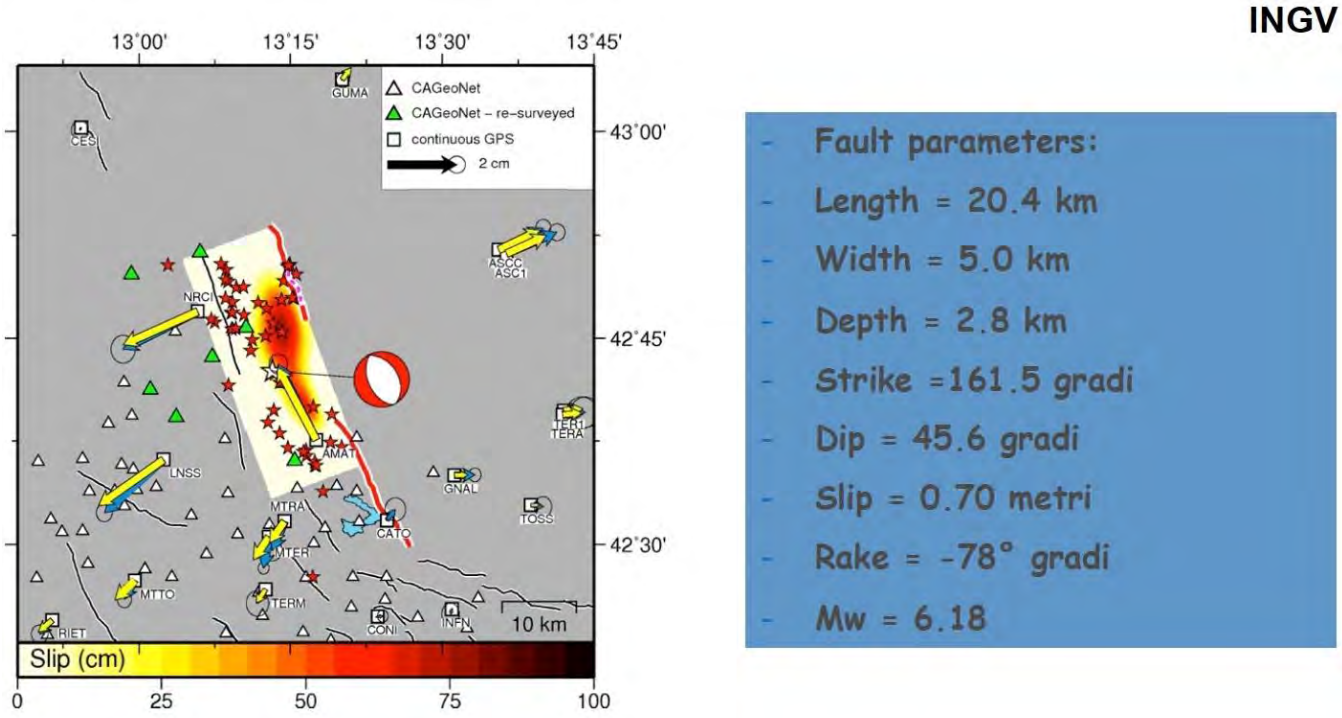

Figure 2.2-2. Source model obtained from the inversion of GPS data.

2.2.3 High rate GPS

High frequency GPS recordings (from 1 to 10 Hz) available for some stations, clearly show the passage of the seismic waves and its associated ground movement (Figure 2.2-3).

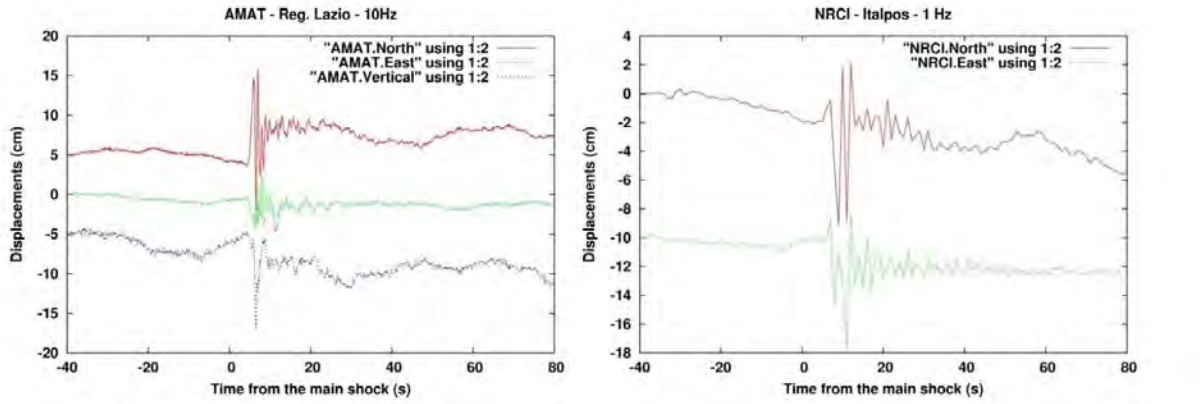

Figure 2.2-3. Left: ground displacement recording at station AMAT at Amatrice. The peak-to-peak values reach 15 cm displacement on the North component and 10 cm on the vertical. Right: at station NRCI at Norcia the peak-to-peak displacement is 15 cm, in the SW direction.

2.2.4 SAR and joint inversion with CGPS data (IREA-CNR & INGV Working group, DOI: 10.5281/zenodo.61682)

Coseismic deformation

The obtained results show that lowering of the land surface, in a typical spoon-shape, extends about 20 km in the NNW direction, confirming the preliminary interferometry analysis (Figure 2.2-4). The maximum vertical ground displacement is about 20 cm near the area of Accumoli. The East component of coseismic displacement points to four areas with alternating displacement, with maximum deformation values of about 16 cm towards West (Figure 2.2-4). More detailed information on local effects could be extracted from displacement maps. These effects are probably linked to slope instability.

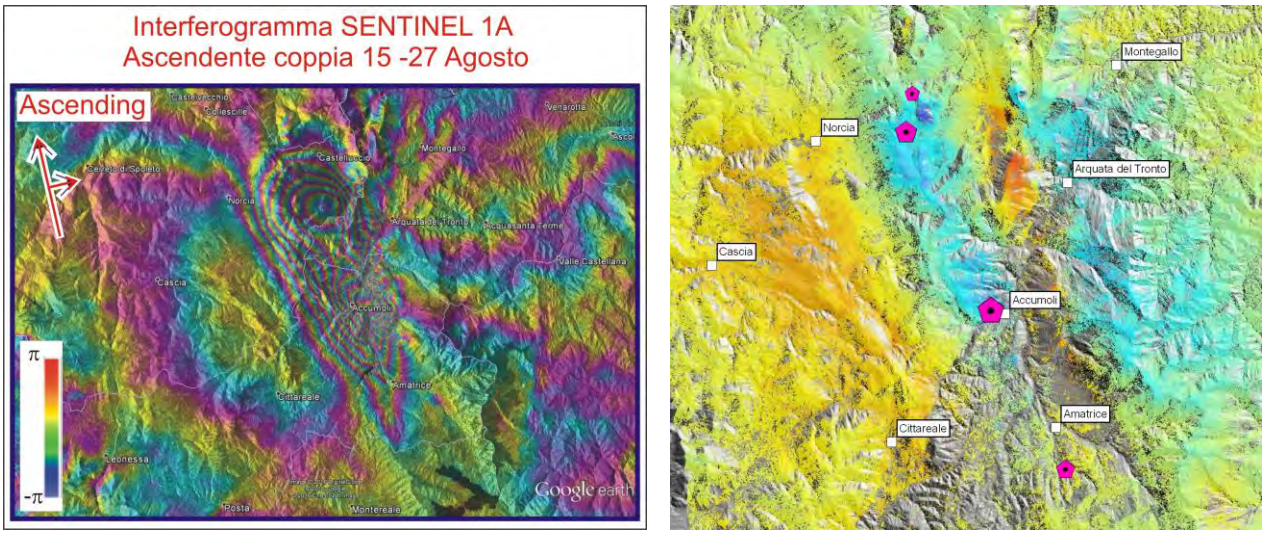

Figure 2.2-4. Left: One of the Sentnel1-A interferograms use in the seismic source modeling with SAR an CGPS data. Right: pattern of the East component as reconstructed from InSAR data of different origin.

SAR-CGPS data modeling

In comparison to the first report (IREA-CNR & INGV Working group, 2016 DOI:10.5281/zenodo.60938), the number of geodetic data sets used for this modeling has increased from one to seven: 6 SAR data sets from 4 different satellites, and one GPS data set. The results of the inversion are therefore quite reliable, and, although the inversion is not constrained by seismological or geological data, they are in strong agreement with them.

A total of 19500 ground displacement values have been inverted. The data set includes several SAR lines of flight and 107 displacement values from CGPS stations (INGV Working group "GPS Geodesy", 2016. DOI 10.5281/zenodo.61355). Modeling was based on the following procedure: ground displacement data obtained by unwrapping the interferograms have been georeferenced and resampled on grid with variable size. The data sets were then modeled through an analytical description (based on Okada, 1985). Fault parameters are evaluated with a non-linear inversion scheme (no parameter has an a priori constraint). The source geometry and the *rake* calculated in with the non-linear procedure were fixed in the following linear inversion, a step used to estimate the slip distribution on the fault plane. A positivity constraint was used (Non-Negative Least Square). Similarly to the first report, separate inversions were executed for the single-source and double-source cases (Tale 2, and Figures 2.2-5 and 2.2-6). Table 2 shows the results of the linear inversion.

La Tabella 2 mostra i parametri delle sorgenti modellate.

Modello	Mw osservata	Magnitudo geodetica	Lunghezza	Larghezza massima	Profondità del tetto	Strike	Dip	Rake	Slip max	RMS medio
Singola faglia	6.0 (+ 5.3)	6.2	~21 km	~9 km	~1500 m	164°	46°	-73°	120 cm	1.4 cm
Doppia faglia - Nord	6.0 (+ 5.3)	6.2	~8 km	~8 km	~3000 m	175°	39°	-65°	140 cm	1.4 cm
Doppia faglia - Sud			~12 km	~5 km	~2500 m	165°	51°	-70°	130 cm	

Nota: i valori indicati di lunghezza, larghezza e profondità sono relativi alle aree di maggiore slip

The two models are very similar and their fit to the data is basically identical (Table 2). It is possible to try to associate the rupture to fault planes that are observed at the surface by prolonging and intersecting the model planes with the topography (Figures 2.2-5 and 2.2-6). The superficial trace of the single-fault model is parallel and almost coincident (within ±800 m) with the Gorzano-Laga-Vettore fault system (Figure 2.2-5). In the two-faults model a similar behavior is observed for the Southern fault, while the trace of the Northern fault rotates towards NE and should emerge at about 3 km East of the Mt. Vettore (Figure 2.2-6). Both models are compatible, within uncertainty, with the aftershock distribution, although a slightly better behavior of the two-faults model is observed in the Northern part of the area. Table 2 shows the rupture dimensions derived from the slip values in the two models. Both models, show a rupture

that from the hypocenter propagates towards the South, and stops just before reaching Amatrice. Additionally, in the two-faults model there is a rupture that propagates towards the North and slip values tend to zero near the middle of the Piana di Castelluccio. The greatest slip is concentrated below a depth of about 6 km in the North, and at 4 km depth in the South. The slip values can be zero at depths less than 1.5-3 km (in the North) or 700 m (in the South), depending on which model is considered. In the more superficial parts of the faults, slip values of a few cm are modeled in a discontinuous way.

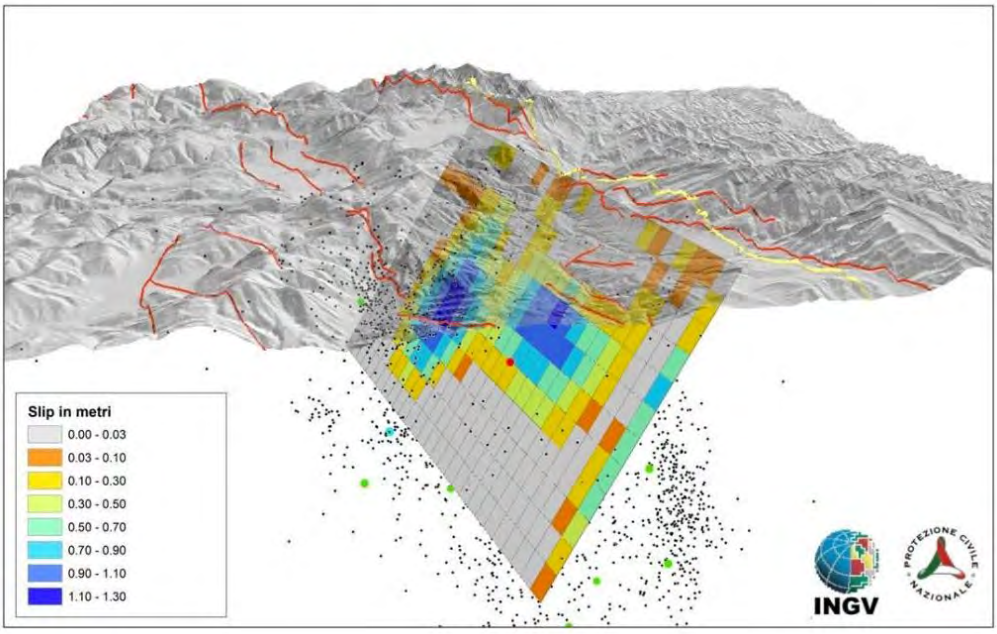

Figure 2.2-5. - 3D representation of the single-fault slip model. The yellow line indicates the intersection of the fault plane with the surface. The red lines are fault traces derived from geological bibliography. The red symbol is the mainshock, the green symbols are the other major shocks recorded up to August 29.

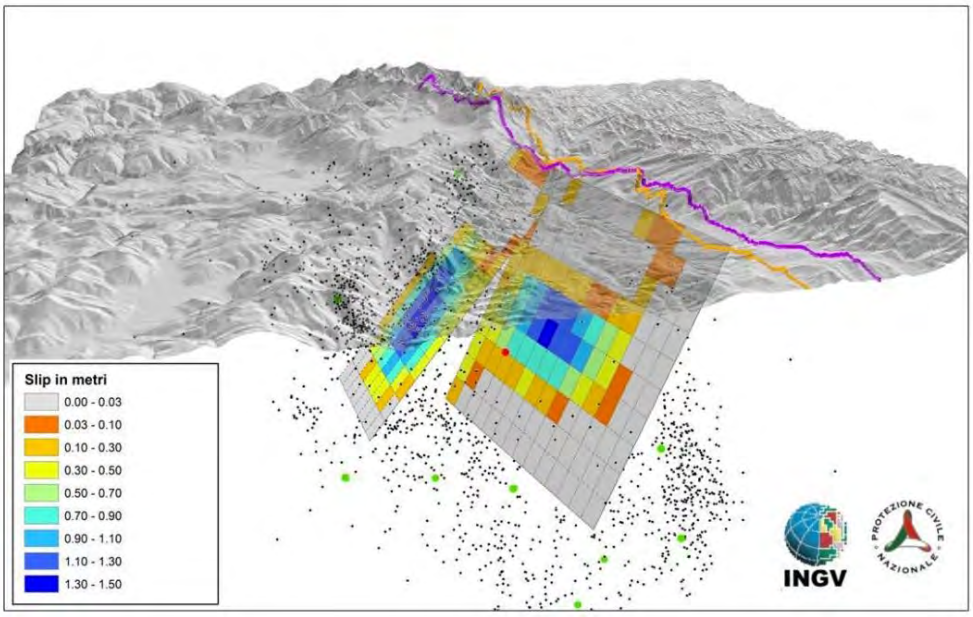

Figure 2.2-6. - 3D representation of the two-faults slip model. The orange line is the intersection of the Northern fault with the surface; the purple line is the intersection of the Southern fault. The red symbol is the mainshock, the green symbols are the other major shocks recorded up to August 29.

Obviously, the dislocation planes derived from the two models are approximations of faults that are likely to have a more complex geometry. As soon as more accurate information on seismicity will be available, it will be possible to better constrain the deep geometry of the sources. A first comparison shows that the *dip* and *strike* of the geodetic sources are very similar to the ones obtained from focal mechanisms and hypocenter patterns, although the latter are affected by significant location errors (mostly due to the use of a preliminary velocity model in the procedure) that might limit this comparison. Small differences between the projections of the planes derived by geodetic inversion and the hypocenter patterns, are within uncertainty. Another important aspect that should be considered is that planar patterns of the aftershock hypocenters could be ascribed to minor faults, or to faults that were reactivated by local stress variations, and thus cannot be associated to the main fault rupture.

2.3 Geology

2.3.1 Superficial ruptures (EMERGEO Working Group)

Starting from the morning of August 24, teams of geologist from EMERGEO (one of INGV groups that operate during an earthquake emergency) began surveying the ground effects of the earthquake. The survey teams are investigating the epicentral area, extending about 40 km between Castelluccio di Norcia, to the North, and Località Ortolano South of the artificial lake of Campotosto. At present, information from 3000 observation points (Figure 2.3-1) have been logged. Numerous fractures along mountain slopes and cultivated fields have been reported (often these deformation features are well visible on paved roads). Landslides, slumps, and collapses of rocks of small-medium dimensions, have also been observed. A superficial and

continuous fracture zone, about 5.2 km long, was observed in the Northern part of the epicentral area, along the southwestern flank of Mount Vettore. The geometric characteristics of the observed deformation features are summarized in Figure 2.3-2.

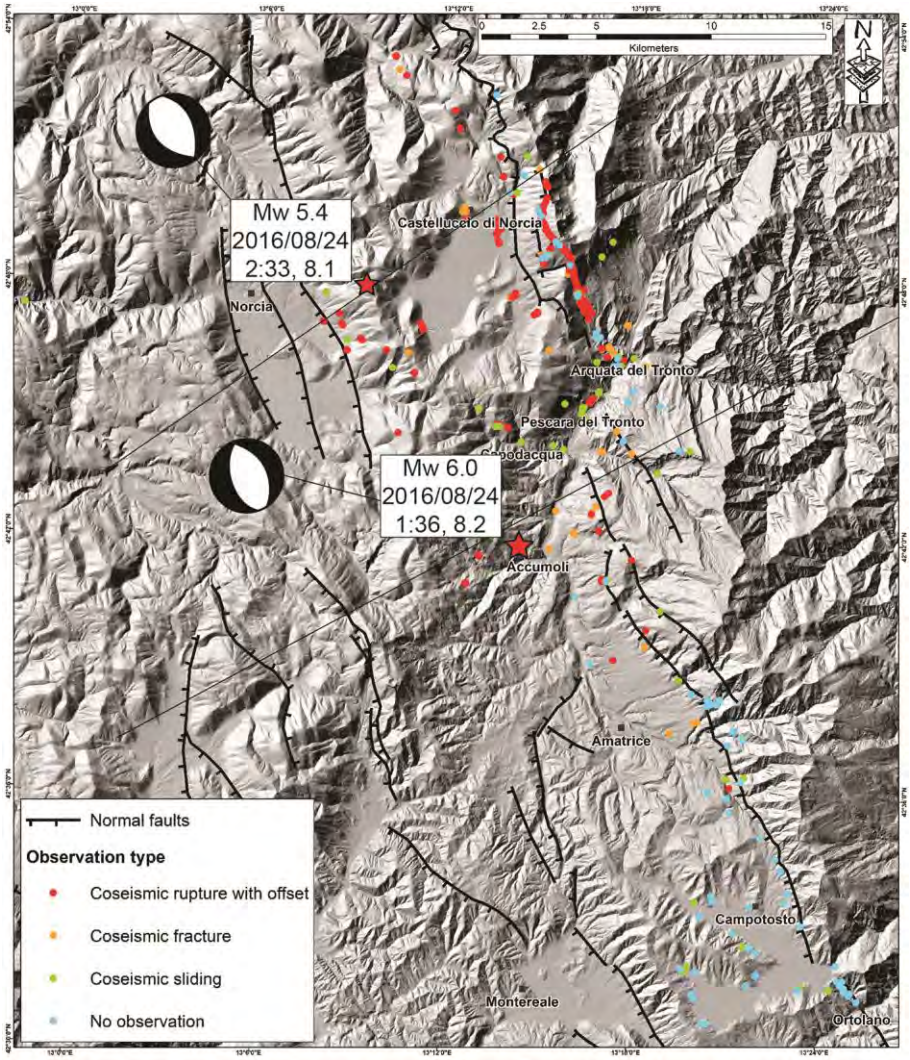

Figure 2.3-1. Map showing the distribution of the 3000 observation points; the faults have been modified from the Mappa Geologica d'Italia scala 1:100.000 (Fogli F132 Norcia e F139 L'Aquila -ISPRA) and from Centamore et al. (1992); the location of the main event was provided by the AMA_LOC Working Group – DOI: 10.5281/zenodo.61404. Coseismic ruptures are shown in orange, landslides/slumps are in green, the absence of coseismic deformation is in light blue. The traces of the geological sections shown in Figure 2.3-3 are in black.

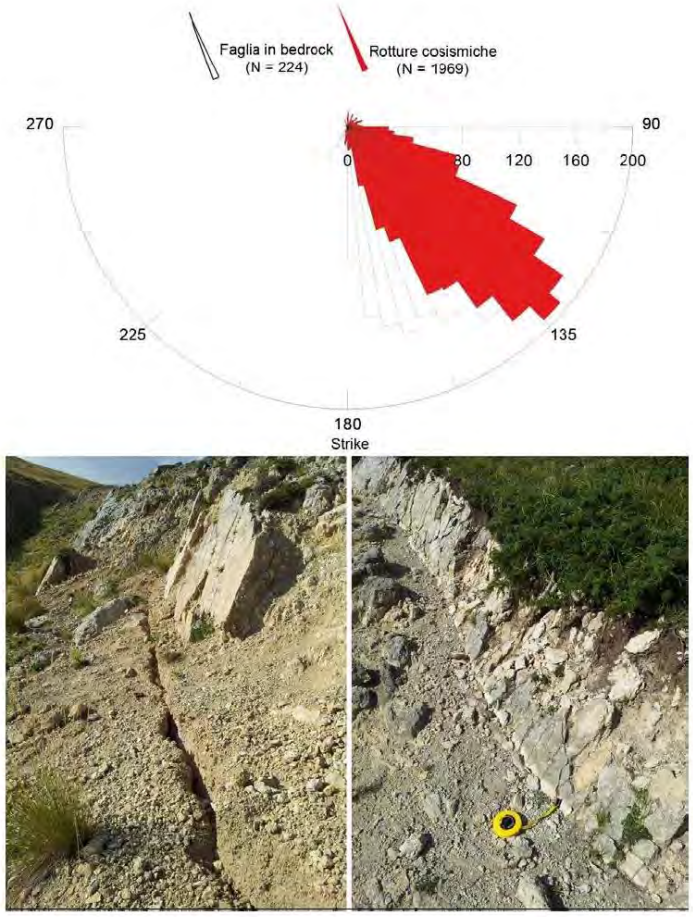

Figure 2.3-2. Upper panel: rose diagram showing the directions of the cosesimic ruptures on the unconsolidated deposits (in red) and along the fault plane within the rock of Mounts Vettore and Vettoretto.

Middle panel: pictures of the fractures.

Lower panel: two histograms showing the vertical (left) and horizontal (right) fault throw observed along the Mts. Vettore and Vettoretto fault, and their respective maps.

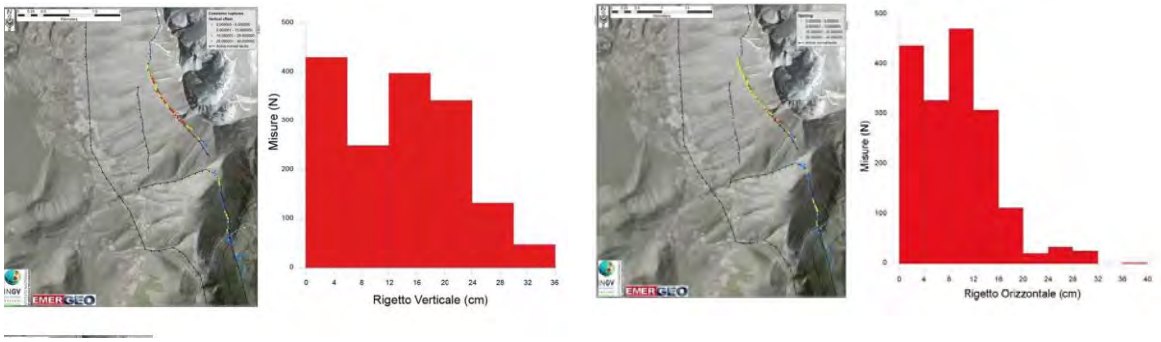

2.3.2 Comparison with geological information

The ongoing seismic sequence that started with the August 24 earthquake, is affecting an area of the central Apennines that is well known in terms of its superficial structural elements. In Figure 2.3-4 the geological sections available for the area are compared with the distribution in space of seismicity. It is noteworthy that seismicity lies along patterns that seem to be a prolongation in depth of the tectonic features identified on the surface. In particular, the more superficial seismicity in the eastern sector seems to delineate the overthrusting of the Sibillini Mts. However, these are preliminary considerations that need the support of a more in-depth analysis.

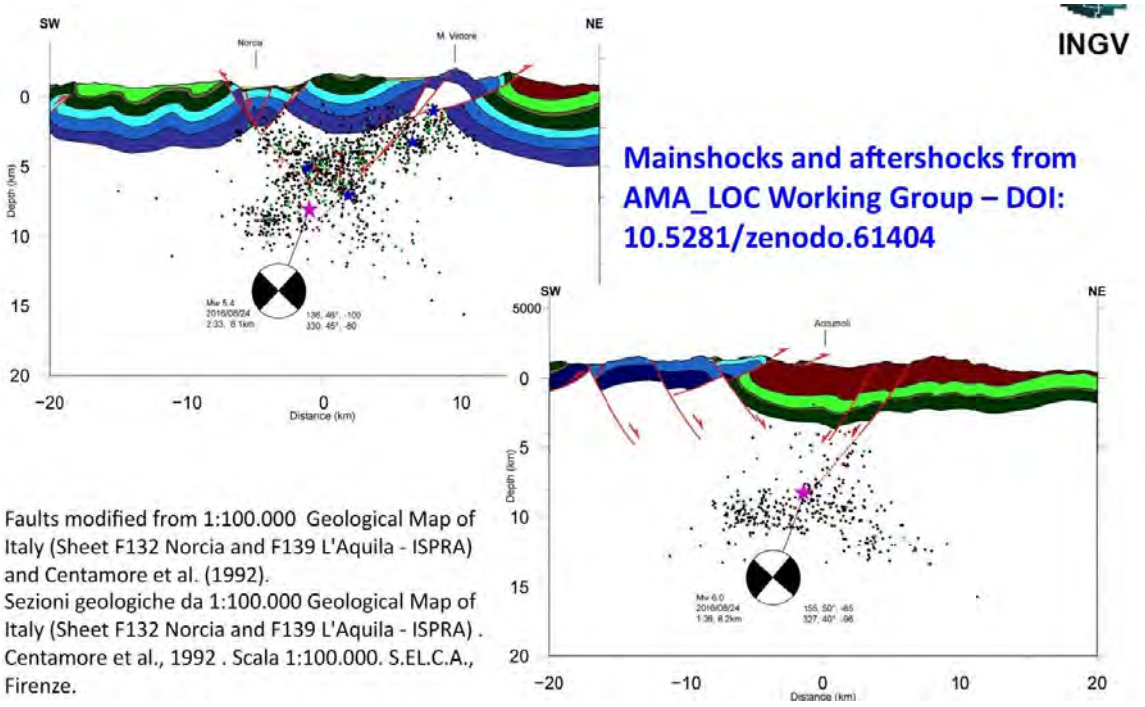

Figure 2.3-3. Geological sections modified after the carta geologica Italiana. Hypocenter locations were provided by the AMA_LOC Working Group – DOI: 10.5281/zenodo.61404.

2.4 Macroseismic study

2.4.1 Macroseismic survey (from the "*Rapporto sugli effetti macrosismici del terremoto del 24 Agosto 2016 di Amatrice in scala MCS"* by P. Galli1, E. Peronace2 e A. Tertulliani 3; *Coordinamento del rilievo macrosismico MCS* edited by P. Galli1 e A. Tertulliani3) (1 Dipartimento Protezione Civile; 2 CNR-IGAG; 3 INGV-QUEST)

Right after the occurrence of the Ml 6.0 earthquake, at 03:36 (CEST) of August 24, at the border dividing the Lazio, Abruzzo, Marche and Umbria regions (Amatrice area, province of Rieti), the macroseismic survey teams from DPC, CNR- IGAG and INGV reached the epicentral area. The mainshock was soon followed by the Nursina Ml 5.3 earthquake. The teams reached the mesoseismic area from different directions, i.e., from NE in the area of Norcia, from the North in the area of Arquata and from the South from Antrodoco. The surveys were carried out fraction by fraction by the different teams, also in the same locations at different times, in order to compare and calibrate the macroseismic observations. The teams met several times on the field to exchange data, impressions and opinions. Other colleagues could communicate their news and reports remotely to the teams. One should keep in mind that a macroseismic survey in MCS scale needs to be executed quickly during an emergency. The survey's main objective is to identify, in the best possible way, the distribution of the medium-high amount of damage on a short time scale (2 days), and the extension of the damaged area within a reasonable time interval (15 days), using a homogeneous and immediately applicable criterion such as the MCS scale. More specifically, the survey is conducted by using the percent damage of the MCS scale (1930), as quantified by Molin (2009), in an increasing progression starting from intensity degrees ≥ V MCS and according to the five levels of damage of the original scale. The classification of the buildings in a residential area according to the vulnerability classes defined by the EMS european macroseismic scale (Grünthal, 1998) is not applicable during an emergency. This was also true for the 2009 L'Aquila earthquake emergency, as it was not possible to assign the vulnerability classes to the buildings with the required confidence and rapidity. This procedure was possible only after carrying out prolonged inspections in the following months (e.g, Molin et al., 2010). The present report does not contain information on the earthquake's after-effects not directly verified by the teams. Up until 8 pm of September 15 a total of 283 sites distributed in 76 municipalities were surveyed. Figure 2.4-1 shows a map with the attributed intensities.

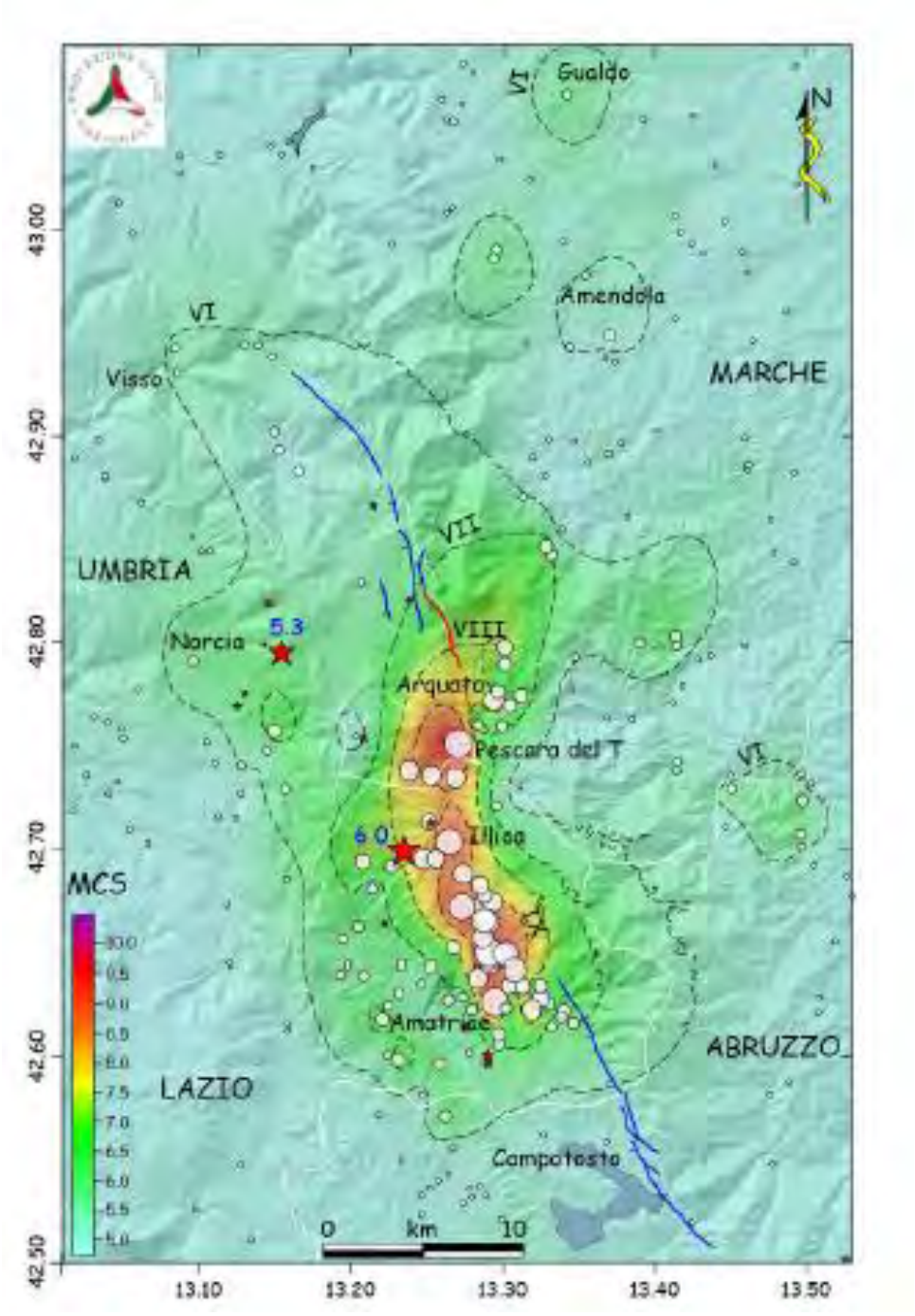

Figure 2.4-1. White circles: observed intensity distribution in the MCS macroseismic scale (the radius is proportional to the intensity value measured at the site). Black dashed lines: isoseisms from VI to IX MCS. Red stars: seismic events with Ml>4 (INGV). Color of the map indicates an approximate areal intensity distribution. In the background: 20 m DTM. Blue lines: Mt. Vettore Fault in the North and Laga fault in the South. Red line: superficial rupture of 2016.

The map from "Hai sentito il terremoto?" ("Did you feel the earthquake?"), derived from a macroseismic questionnaire, is also reported in Figure 2.4-2.

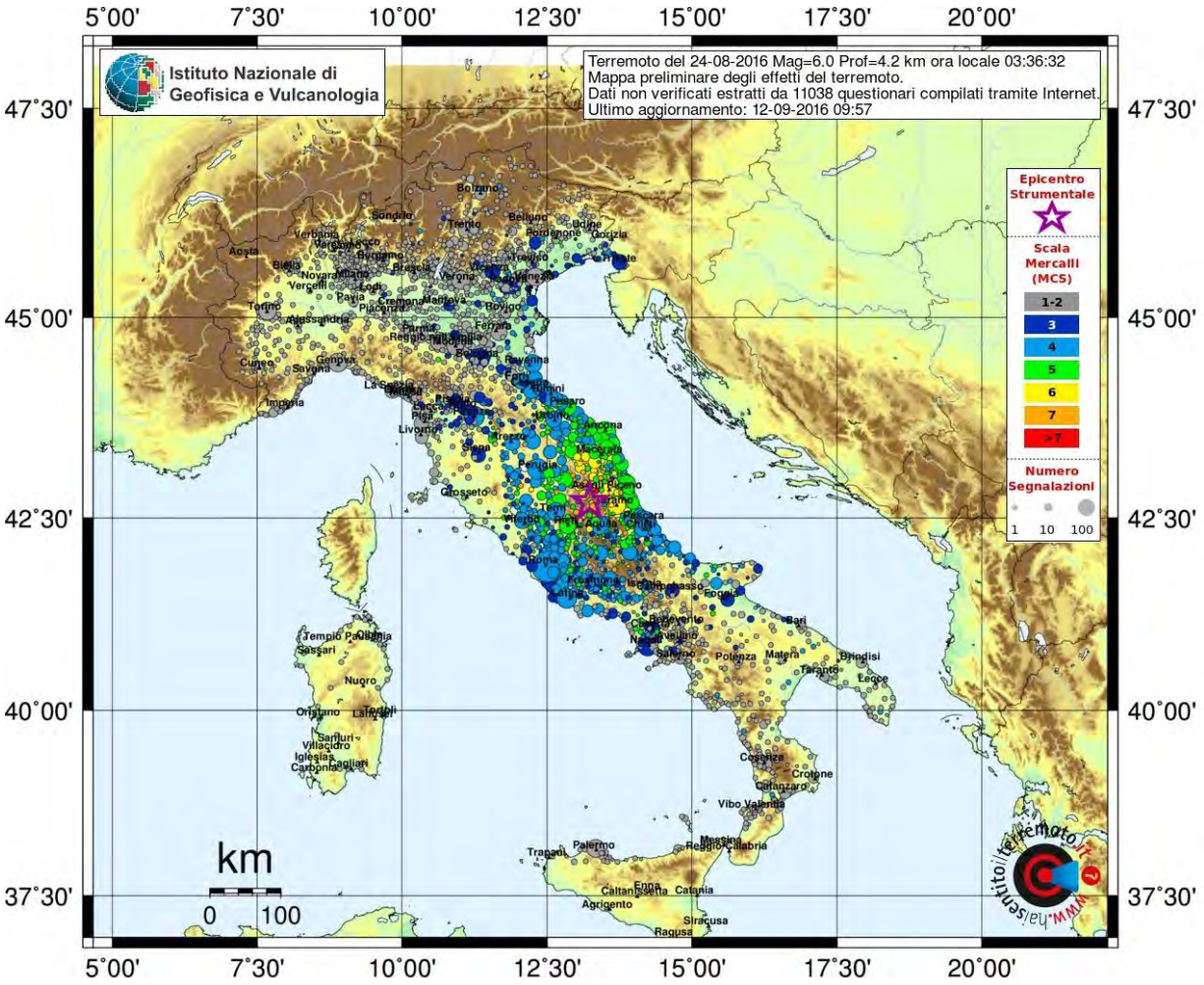

Figure 2.4-2. Seismic intensity map in MCS scale (Mercalli-Cancani-Sieberg) showing how the effects have been felt on the Italian territory. The map is based on thousands of reports obtained from the population through a web-based questionnaire. The map includes a legend (on the right). The purple star indicates the main event's instrumental epicenter, the colored circles indicate the intensities associated to every municipality. The header includes earthquake parameters: date, magnitude (Ml), depth (Prof) and local origin time. The header also includes the number of questionnaires used to produce the map.

3 Overall interpretation

In the three weeks following the Amatrice earthquake of August 24, 2016, many surveys have been conducted to collect a variety of data. Furthermore, dense monitoring networks have been installed to measure geophysical parameters: seismic, geodetic, and others. The seismic surveillance room could benefit from the supplementary data transmitted in real time from the new seismic stations installed in the area affected by the seismic sequence. These data permit a more accurate calculation of the earthquakes' hypocentral parameters. On the basis of the numerous observations collected in the affected area (seismological, geodetic and geological) and the increase of knowledge on the seismogenic process, it is possible to propose a second preliminary overall interpretation.

The main M_L 6.0 event of August 24 was caused by the slip of an extensive fault with strike ≅156° and dip ≅50° towards SW. The length of the fault is about 20-25 km. Starting from the nucleation point of the earthquake, the rupture was bilateral (towards NW and SE) with two areas of slip concentration on the fault plane. The duration of the rupture was about 6 s. Deformation features that are likely due to "surface ruptures", have been surveyed and mapped along the well-known Mt. Vettore fault. A scientific debate is taking place to discriminate the origin of these ruptures, by establishing if they are a direct superficial expression of the fault responsible for the earthquake, or secondary deformation features. In the following months the focus will be on how the preexistent geological structures, inherited from the previous compressional tectonic regime, might have influenced the geometry of the fault system that was activated. Section 2.3.2 Comparison with geological information, is a first view that suggests interesting interpretative elements. The comparison between observations and results coming from different types of data allows for a more accurate description of the seismic phenomena. In fact, by superimposing the hypocentral locations described in paragraph *1.3 Fault geometry derived from the hypocenter locations (AMA_LOC Working Group – DOI: 10.5281/zenodo.61404)* to the source model derived from the accelerometric data shown in *2.1.1 Inversion of Strong Motion data (DOI 10.5281/zenodo.61460)*, one can see that the fault areas with the highest slip values also contain a smaller number of aftershocks (this is particularly true for the southernmost high slip patch, see Figure 3-1, left panel). Furthermore, the aftershocks with higher magnitude (M_L>3.0) tend to concentrate along the edges of the high slip areas (Figure 3-1, right panel).

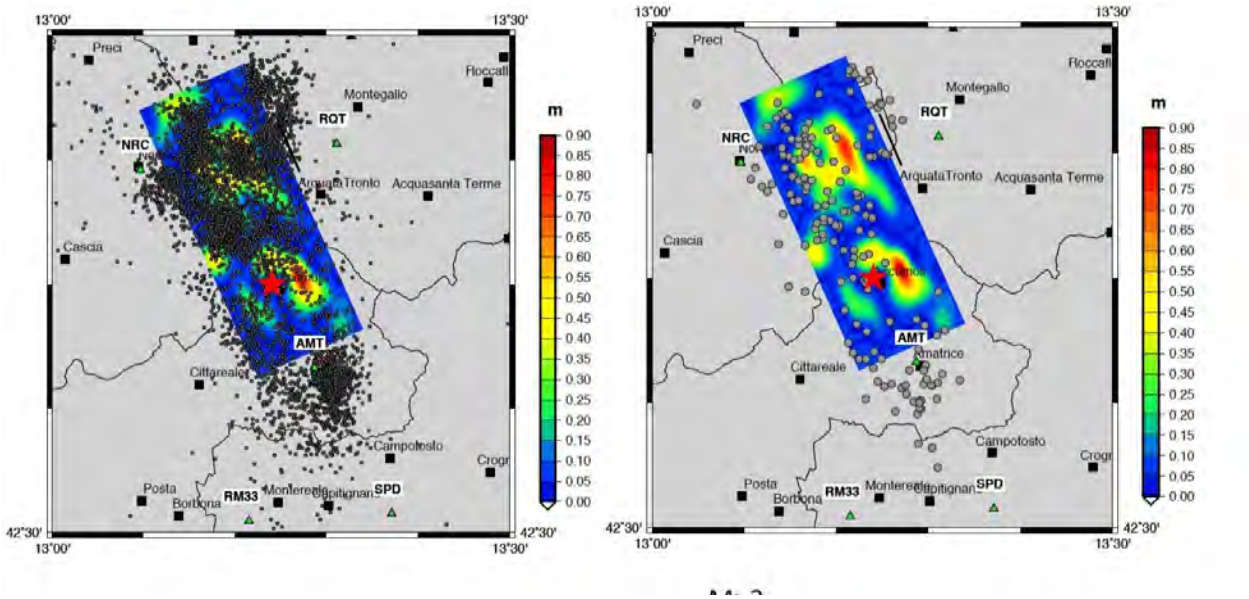

Figure 3-1. Comparison between aftershock location and slip pattern on the main fault plane. The source model in figure is the one derived from the inversion of accelerometric data (DOI 10.5281/zenodo.61460). In the left panel all relocated aftershocks are shown, while in the right panel only aftershocks with magnitude > 3 .

Thanks to the deployment of dense networks it was possible to follow the evolution of the sequence. In its spatio-temporal evolution the sequence activated fault segments adjacent to the modeled one: to the North the Mt. Vettore fault and several antithetic structures that dip towards NE, to the South the northern portion of the Mt. Gorzano fault. The southern portion of the Mt. Gorzano fault had been previously activated by the aftershocks of the 2009 L'Aquila earthquake. It is possible that other damaging earthquakes might be generated on these adjacent faults. To better understand how the August 24 earthquake has modified the local stress field, the model derived from geodetic data was applied to calculate the Coulomb stress field changes (Coulomb Failure Function, CFF) on the nearby faults. The geometry of the nearby faults is described on the basis of the August 24 fault. Figure 3-2 shows the result of this calculation (considering the two-faults SAR-GPS model) on the presumed planes of the six closest faults (faults geometry provided by Emergeo). Significant positive values of CFF, up to 0.5-0.6 Mpa, are associated to the NW limit of the Mt. Gorzano fault, that was affected, after the mainshock, by intense low-magnitude activity. Much lower values of CFF are associated to the Vettore-Bove fault, in the North, although it is possible that the chosen fault plane might not be realistic since it is not in continuity with the Vettore fault. If the fault plane continued to the SE, than it is likely that there would be a CFF distribution similar to the one calculated for the Gorzano fault**.**

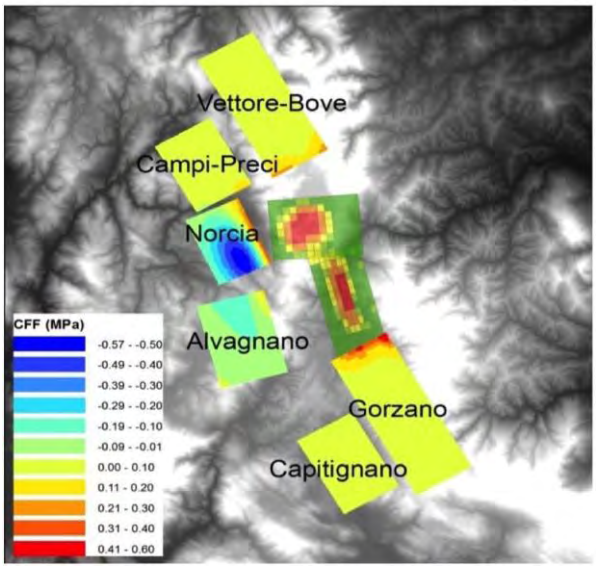

Figure 3-2. Distribution of the Coulomb Failure Function (CFF) on the nearby structures, as caused by the dislocation of the two-faults model. Fault planes of the nearby structures provided by the Emergeo Group (DOI: 10.5281/zenodo.61682).

The seismic sequence affected a volume that corresponds to a mass of about 2500 billion tons. The gravitational potential energy freed from the collapse of this volume of superficial crust (*graviquake*) is equivalent to 10^{16} joule, at least 100 times greater than the released seismic (elastic) energy. This means that the majority of the gravitational energy was dissipated as fracturing and heat due to friction. SAR data show a coseismic collapse, i.e., lowering of the ground surface, of about 20 cm in the area where the greatest damage was recorded (Figure 3-3).

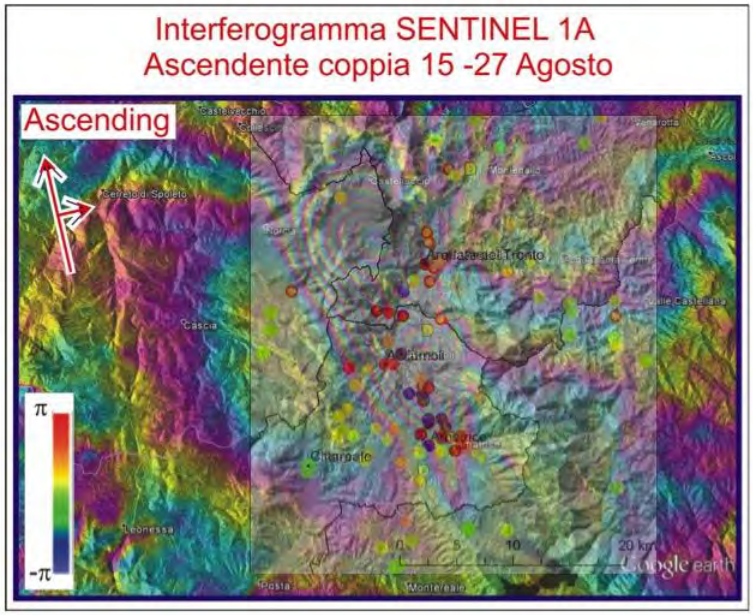

Figure 3-3. Damage data have been superimposed on SAR data. Damage is concentrated in the area subjected to subsidence.

Disclaimer and limits of use of information

The INGV, in accordance with the Article 2 of Decree Law 381/1999, carries out seismic and volcanic monitoring of the Italian national territory, providing for the organization of integrated national seismic network and the coordination of local and regional seismic networks as described in the agreement with the Department of Civil Protection.
INGV contributes, within the limits of its skills, to the evaluation of seismic and volcanic hazard in the Country, according to the mode agreed in the ten-year program between INGV and DPC February 2, 2012 (Prot. INGV 2052 of 27/2/2012), and to the activities planned as part of the National Civil Protection System.

In particular, this document[1] has informative purposes concerning the observations and the data collected from the monitoring and observational networks managed by INGV.
INGV provides scientific information using the best scientific knowledge available at the time of the drafting of the documents produced; However, due to the complexity of natural phenomena in question, nothing can be blamed to INGV about the possible incompleteness and uncertainty of the reported data.

INGV is not responsible for any use, even partial, of the contents of this document by third parties and any damage caused to third parties resulting from its use.

The data contained in this document is the property of the INGV.

This document is level 3 as defined in the "Principi della politica dei dati dell'INGV (D.P. n. 200 del 26.04.2016)".